Journal of Applied Polymer Science

Investigating the thermal, mechanical, and electrochemical properties of PVdF/PVP nanofibrous membranes for supercapacitor applications

A. Jabbarnia,[1] W.S. Khan,[2] A. Ghazinezami,[1] R. Asmatulu[1]

[1]Department of Mechanical Engineering, Wichita State University, Wichita, 1845, Fairmount Kansas 67260-0133

[2]Department of Mechanical and Industrial Engineering, Majmaah University, P.O. Box. 66, Majmaah, Saudi Arabia

Correspondence to: R. Asmatulu (E-mail: ramazan.asmatulu@wichita.edu) and A. Jabbarnia (E-mail: a.jabbarnia@gmail.com)

ABSTRACT: Polyvinylidene fluoride and polyvinylpyrrolidone polymers incorporated with carbon black nanoparticles (50 nm) were electrospun to fabricate nanofibrous membranes for supercapacitor separators. Different weight percentages (0, 0.25, 0.5, 1, 2, and 4 wt %) of carbon black nanoparticles were dispersed in *N,N*-dimethylacetamide and acetone prior to the electrospinning processes at various voltage, pump speed, and tip-to-collector distances. The morphology, thermal, mechanical, hydrophobic, and electrochemical characterization of nanofibrous membrane were analyzed using different techniques, such as scanning electron microscopy, differential scanning calorimetry, capacitance bridge, thermogravimetric analysis, dynamic mechanical analyzer, and water contact angle. Effects of annealing and UV irradiation exposures on the nanofibrous membranes were investigated in detail. Test results revealed that the physical properties of the nanocomposite separators were significantly enhanced as a function of carbon black inclusions in the polymeric structures, which may be useful for the applications of supercapacitor separators and other energy storage devices.
 J. Appl. Polym. Sci. **2016**, *133*, 43707.

KEYWORDS: electrospinning; fibers; membranes; nanostructured polymers; thermal properties

Received 13 September 2015; accepted 27 March 2016

DOI: 10.1002/app.43707

INTRODUCTION

New-generation energy storage devices have been receiving considerable attention recently due to the skyrocketing prices of fossil fuel and the desire to meet the ever increasing demand of energy. These devices can be used as backup source devices due to their long cyclic lives with a high charging-discharging rate, excellent power density, low electrical resistivity, and large surface area compared to conventional capacitors and batteries. They have displayed remarkable performance in a wide range of applications such as power backup in some electrical devices and as a power source for hybrid vehicles.[1–6] Research on novel energy storage devices has been considered in order to replace batteries, which have slow discharge rates and a high energy density. Accordingly, it is important to develop storage devices having high energy density and high power density.[7] Supercapacitors are energy storage devices having intermediate features between batteries and traditional capacitors. They can be charged and discharged a number of times without suffering the effects of aging. Supercapacitors work well under hot and cold temperatures. Under normal conditions, a supercapacitor fades very little after being used for several years. In supercapacitors, the capacitance performance depends largely on the electrolyte/electrode and separator. Different types of materials have been used to fabricate separators/electrodes for supercapacitors, such as metal-based oxides and carbonaceous compositions. Carbon-based compositions such as porous carbon, activated carbon fibers, carbon aerogels, carbon nanotubes, and graphene are the most-often-used substances for supercapacitors.[6–10] Carbon-based nanocomposites with conducting polymers have high capacitance values and better cyclic performance in supercapacitors. They also possess high capacitance values due to their functional groups containing phosphorus, nitrogen, and oxygen, which are referred to as the pseudocapacitance effect.[10]

The search for alternating energy sources is a vital concern and a challenging issue. Although, wind, solar, fuel cells, and nuclear energy have been around for several decades, exploiting these sources on a large-scale requires addressing many obstacles. As a result, increased attention has been given to the electrospinning process for fabricating a nanofibrous membrane for application in a supercapacitor. Electrospinning is a unique process used to fabricate continuous nanosize fibers by using a high-voltage power supply. Nanowoven webs have received significant attention because of the prominent characteristics of these electrospun fibers, such as small diameter ranges, high porosity of the structure, and high surface area. This process is less expensive and simple. Owing to these useful properties, many polymers have been utilized to fabricate fibers that can be employed in a variety of

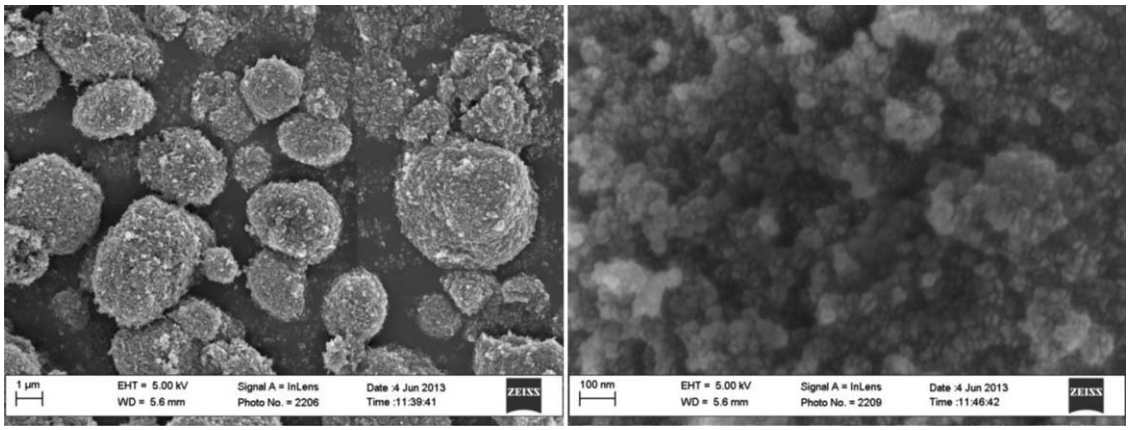

Figure 1. SEM images of carbon black (ELFTEX8) powder at low (left) and high (right) magnifications.

applications such as thermal isolation, membrane separation, and filtration.[11,12] These fibrous membranes contain fully interconnected open cavities with sufficient porosity.[13]

Among many polymers, fluorine-containing materials, such as polyvinylidene fluoride have good mechanical, electrochemical, and thermal stability properties.[14,15] PVdF is a semicrystalline polymer with different forms and complicated microstructures. Due to its high electrical and mechanical properties, PVdF has many significant technological and commercial applications, including membrane separators, fuel cells, biomedical uses, and nonlinear optics, and it is also being used in pyroelectric and piezoelectric materials.[16] PVdF contains various phases, the most common one being the α-phase. The pyroelectric and piezoelectric features of the β-phase of PVdF provide better material properties.[17] Highly conductive carbon black material is described as a highly branched and open structure with small particle size and high porosity. The surface area of carbon black is commonly considered to be more accessible than other types of high-surface-area carbon (1500 m^2 g^{-1}).[18]

Lewandowski *et al.*[19] studied the electrochemical performance of a totally solid state electric double-layer capacitor using a polymer electrolyte and an activated carbon powder as electrode material in which polymer electrolyte serves as separator as well as electrode material. Sivaraman *et al.*[20] reported all-solid-supercapacitor based on chemically synthesized polyaniline (PANI) and sulfonated polymers having fluorinated ethylene propylene copolymer grafted with acrylic acid and sulfonated (FEP-g-AA-SO3H) membrane (separator). Electrospun polymers such as polyvinylidene fluoride (PVdF) and polyacrylonitrile (PAN) and many other, can be used as nanofiber mats in separator applications in electronic devices.[21] These separators provide nanoporous structure leading to increased ionic conductivity of membrane soaked with liquid electrolyte.[21] A uniform electrospun PVdF membrane thickness can be achieved using high polymer concentration and carrying out electrospinning at high voltage. This provides mechanical strength and also results in charge and discharge capacities that exceed many commercially available separators.[21] Karabelli *et al.*[22] prepared PVdF separators for supercapacitor applications, and studied the different properties of PVdF separator such as thermal, mechanical and ionic conductivity. Polymeric materials are widely used as separators and as electrodes in batteries and in ultracapacitors.

High crystallinity of PVdF generally impedes conductivity. Therefore, PVP was added in polymeric solution in order to account for conductivity limitation caused by PVdF high crystallinity and also it increases electrospinnability of polymeric solution. Conventional capacitor technology has focused on minimizing the area of electrode plates and then combining these plates with thin layers of insulating separator having high dielectric constant possibly resulting in high capacitance values.[23] This methodology has certain limits, as separator film can be of minimum thickness before it fails and there are also limits on the dielectric constant of film material.[23] Using the electrospun PVdF and PVP membranes incorporated with carbon black not only increase the surface area of separator and wettability, but also provide the mechanical stability to the separator and increase the dielectric constant values of separators, as well. The main purpose of this study was to fabricate electrospun PVdF/PVP-based separators of supercapacitors and investigate their thermal properties, and the effect of annealing and ultraviolet irradiation on their dielectric constant and surface wettability.

EXPERIMENTAL

Materials

PVdF and PVP with molecular weights of 180,000 and 120,000 g mol^{-1}, respectively, were purchased from Sigma-Aldrich and used without any modification or purification. Carbon black (ELFTEX8) was purchased from Cabot Company and used as reinforcement nanoparticles. *N,N*-dimethylacetamide (DMAC) and acetone, were purchased from Fisher Scientific and used as a solvent. Figure 1 shows SEM images of the carbon black powder used in this experiment. The size of the reinforcement nanoparticles was around 60 nm.

Nanofiber Fabrication

Various weight percentages (0, 0.25, 0.5, 1, 2, and 4 wt %) of carbon black nanopowders were dispersed in the DMAC/acetone solvent and sonicated for 90 min; then PVdF and 2 wt % of PVP were added separately to the dispersions. Ratio of 80:20 was

chosen during the dispersion and dissolution processes. The solution was constantly stirred at 550 rpm and 60 °C for 5 h before the electrospinning process. The dispersed solution was transferred to a 10 mL plastic syringe connected to a capillary needle having an inside diameter of 0.5 mm. The electrospinning parameters of voltage, distance between tip and collector, and syringe pump speed were 25 KV (DC), 25 cm, and 2 mL h^{-1}, respectively. Electrospun fibers were then collected on an aluminum screen and dried in an oven at 60 °C for 8 h to remove all residual solvents.

Characterization

The morphology of the nanofibers samples was observed using a field-emission scanning electron microscope (Oxford Instruments). Before SEM observations, the samples were coated with gold spatter. The thermal properties of samples were analyzed using a differential scanning calorimeter (TA Instruments Q400). Thermal stability of the nanofibers was carried out under a nitrogen flow using thermogravimetric analyzer (TA Instruments Q5000). The rate of temperature increase during the test was 10 °C min^{-1} in the temperature range of 50–1000 °C. Dynamic mechanical properties of the electrospun nanofibers were evaluated using a dynamic mechanical analyzer (TA Instruments Q800) on compression-molded films 25 × 5 × 0.5 mm^3 in size. Dynamic tests were conducted between room temperature and 180 °C at a heating rate of 5 °C min^{-1} and a frequency of 1 Hz.

RESULTS AND DISCUSSION

SEM Images

SEM images of the PVdF/PVP nanofibers incorporated with carbon black nanopowders are shown in Figure 2. As can be seen, all nanofibers are nanosize with diameters ranging from 100 to 200 nm. A good combination of PVdF/PVP and carbon black nanopowders is observed in all samples. Some round-shaped beads were formed during electrospinning, especially in the 4 wt % carbon black sample, which may have been due to high carbon loading. Matlab software was employed to analyze the porous structures of the PVdF/PVP nanofibers. The image histogram of the samples indicates that all nanofibers surfaces have approximately 15–20% porous structures.

Thermogravimetric Analysis

Thermogravimetric analysis is a useful tool to evaluate the mass changes of PVdF/PVP nanofiber samples. TGA was utilized to investigate the thermal stability of the electrospun fibers. The samples were heated from 50 to 1,000 °C in a nitrogen atmosphere at a heating rate of 10 °C min^{-1}. Figure 3 shows the TGA thermograms of PVdF/PVP samples with 0, 0.25, 1, 2, and 4 wt % carbon black nanopowders. According to the results, all nanofibers underwent single-step degradation between approximately 440 and 450 °C. For pure PVdF, generally initial degradation occurs at 400 °C.[24] Addition of carbon black provides initial stability and PVdF/PVP shows high stability up to 450 °C.[25–29] Electrospun nanofiber samples containing carbon black nanopowders underwent continuous weight loss after 450 °C. Curves of the PVdF/PVP polymers with varying degrees of carbon black showed a satisfactory thermal stability. The weight loss at higher temperatures is due to the polymer's thermal breakdown. The initial decomposition temperature of PVdF/PVP with 4 wt % carbon black content was at 450 °C. However, no appreciable thermal stability was observed in all samples and the weight loss pattern and corresponding temperatures were almost similar to pure PVdF/PVP sample. As initially expected, carbon black failed to provide appreciable thermal stability. However, some initial thermal stability was observed in all samples compared to pure PVdF.[24]

Differential Scanning Calorimetry

The samples were sealed in an aluminum pan (TA Instruments), and measurements were conducted in the temperature range of 120 to 220 °Cwith a heating rate of 5 °C min^{-1}. A predetermined weight of each sample was used in this experiment. The DSC heat flow and temperature were calibrated using an indium standard. Figure 4 shows DSC thermograms of the samples, indicating endothermic peaks in all samples. As can be seen, the melting temperatures of α, β, and γ phases of PVdF are 165–170, 172–177, and 187–192 °C, respectively.[30–32]

The broad endothermic peak at 166–167 °C indicates the presence of the α-phase for all samples. The PVdF nanofibers mainly contain the α-phase. Adding carbon black to PVdF samples shows the presence of the β-phase, due to the small endothermic peaks at 174–175 °C. The carbon content in PVdF nanofibers may stabilize the β-phase in the structure. The glass transition temperature of the PVdF/PVP nanofibers samples was measured by using the DSC results. Universal V4.5A software from TA Instruments was used to detect the melting temperatures of nanofibers, as shown in Table I. As can be seen, these temperatures were slightly enhanced by increasing the carbon black contents in the polymer matrix. The maximum melting temperature for PVdF/PVP + 4 wt % Carbon black was 169.34 °C. Adding carbon black also enhanced the melting temperature of the PVdF/PVP nanofibers. This was probably due to the presence of carboxyl and hydroxyl groups on the carbon black, which may have caused the plasticization effect or changing the microstructure of the PVdF matrix after being incorporated with carbon black nanopowders.[33] At higher loadings of carbon black, the increased interfacial interactions between C/C and C/polymer led to the formation of the interconnected structure in the polymer composites.[26]

Crystallinity Degree of Nanofibers. Differential scanning calorimetry measurements were carried out to investigate changes in the thermal properties, the enthalpy (heat) of fusion, and crystallization. The heat of fusion (ΔH_f) was obtained from the area under the melting thermogram. The percentage (%) crystallinity (X_c) of the sample can be given by[34]:

$$\%\text{Crystallinity} = \frac{\Delta H_f}{\Delta H_{f(crys.)}} \times 100 \quad (1)$$

where ΔH_f is the heat of fusion of the sample, and $\Delta H_{f\,(crys)}$ is the heat of fusion of 100% crystalline PVdF taken at 104.7 J g^{-1}.[34] The content of PVP and carbon black powders was diminutive in the samples, and both had an amorphous structure.[35,36] Accordingly, for PVdF samples, the crystallinity percentage was calculated by dividing the recorded ΔH_f by the weight fraction of PVdF in the investigated sample. However, carbon black and PVP have amorphous structures, and the addition of small fractions of both would have little effect on the crystallinity of the PVdF polymer. The wide endothermic peaks at 166–167 °C in the DSC results demonstrate the presence of the α-phase for PVdF/PVP samples.

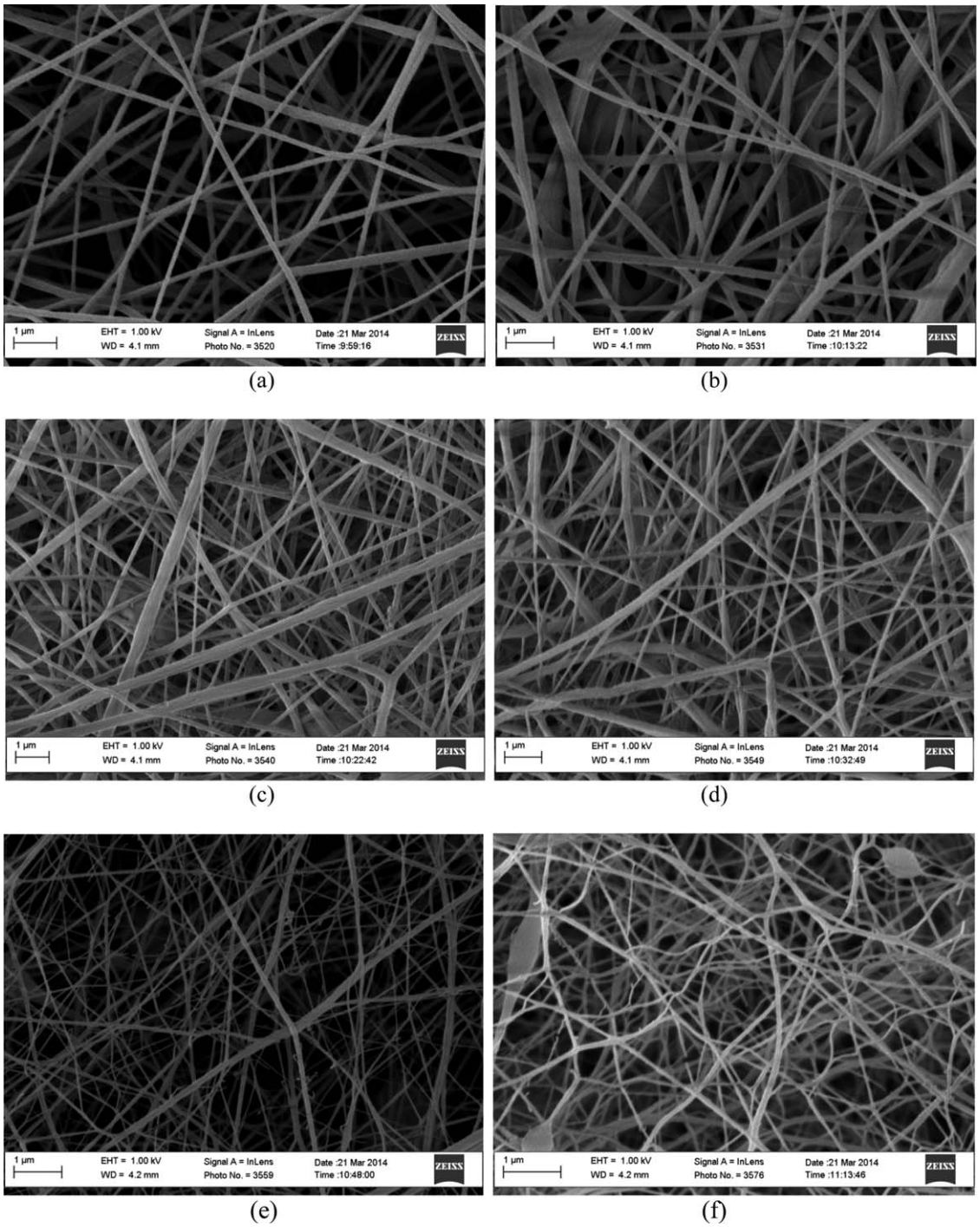

Figure 2. SEM images: (a) electrospun PVdF/PVP fibers, and incorporated with (b) 0.25 wt %, (c) 0.5 wt %, (d) 1 wt %, (e) 2 wt %, and (f) 4% carbon black.

Crystallinity of the α-phase of nanofibers samples are shown in Table II. Crystallinity of the α-phase in electrospun PVdF/PVP increased from 52.44 to 67.91 by adding 1 wt % of carbon black. After adding the higher content of carbon black nanopowders (4 wt %) to the polymer matrix, crystallinity was decreased to 54.59. However, the crystallinity values of 2 and 4 wt % carbon black were still higher than pure PVdF/PVP.

As can be seen, the crystallinity of PVdF/PVP nanofibers increased from 52.44 to 67.91% by adding 1 wt % of carbon black. After adding a higher content of carbon black nanopowders (4 wt %) to the polymer matrix, crystallinity was decreased to 54.59%. However, the crystallinity values with 2 and 4 wt % of carbon black were still higher than pure PVdF/PVP. Reduction in crystallinity of the α-phase in the samples having a

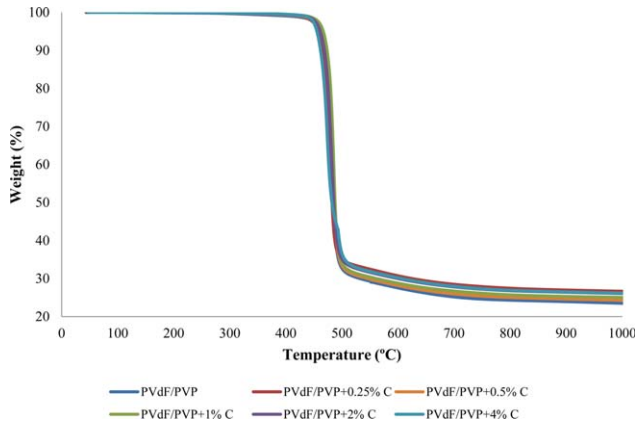

Figure 3. TGA thermogram: PVdF/PVP, and incorporated with 0.25 wt %, 0.5 wt %, 1 wt %, 2 wt %, and 4 wt % carbon black. [Color figure can be viewed in the online issue, which is available at wileyonlinelibrary.com.]

higher content of carbon black nanopowders might be the result of the existence of the β-phase in the structure. The small endothermic peak around 175 °C confirms the presence of the β-phase in PVdF/PVP with 2 and 4 wt % carbon black nanopowder samples, which results in decreasing the crystallinity of the α-phase.

Dynamic Mechanical Analyzer

The dynamic mechanical spectrum of polyvinylidene fluoride has been extensively studied.[37] The dynamic mechanical properties of PVdF/PVP samples were studied on films 25 × 5 × 0.5 mm^3 in size. Dynamic response tests were carried out from room temperature to 180 °C at a heating rate of 5 °C min^{-1}. The storage modulus (E'), loss modulus (E''), and tan δ of PVdF/PVP nanofibers with different carbon black percentages were determined. Figures 5–8 show the DMA curves of the E', E'', and tan δ of the PVdF/PVP with 0, 1, 2, and 4 wt % of carbon black, respectively. These

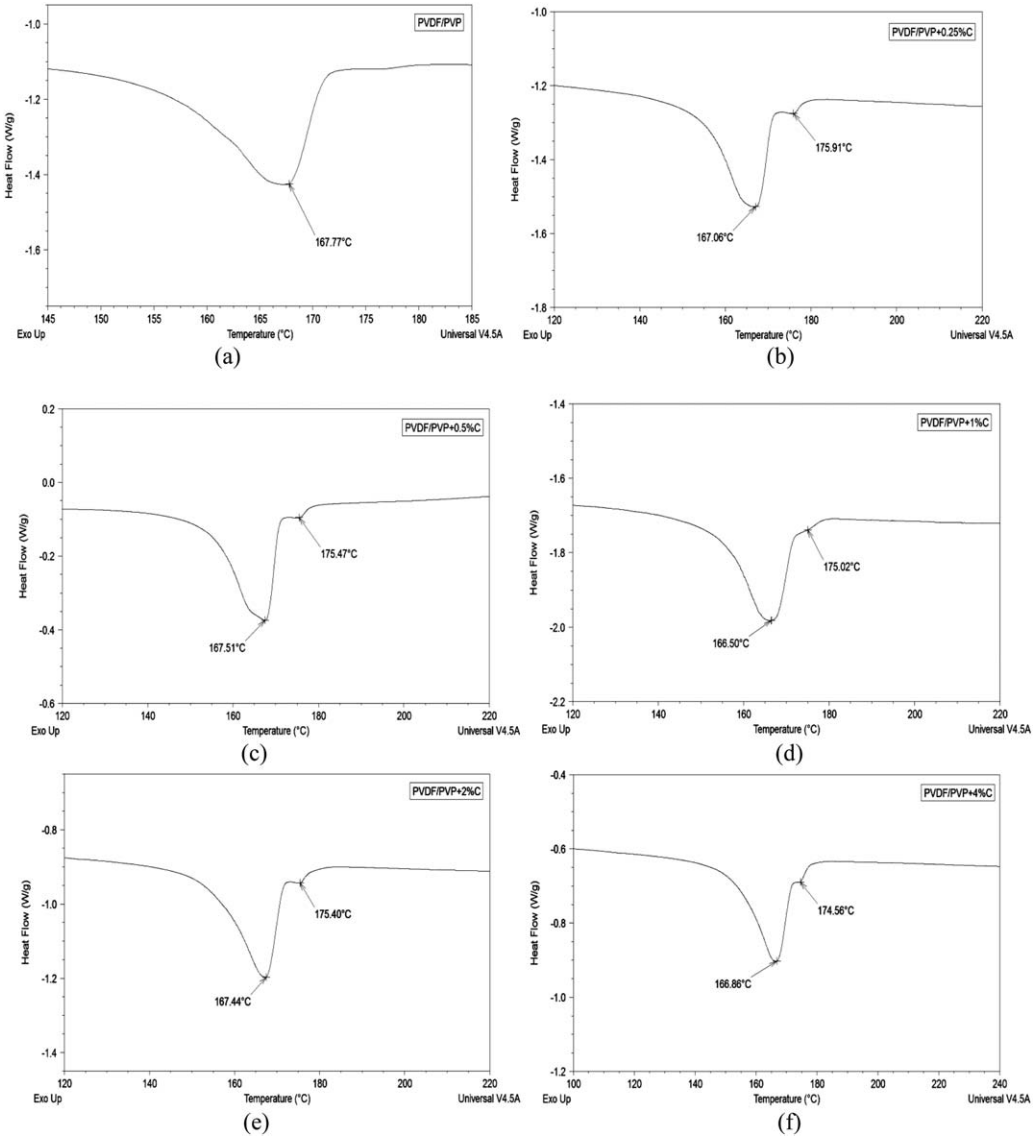

Figure 4. DSC results: (a) PVdF/PVP, and incorporated with (b) 0.25 wt %, (c) 0.5 wt %, (d) 1 wt %, (e) 2 wt %, and (f) 4 wt % carbon black.

Table I. Melting Temperatures of PVdF/PVP Nanofibers

Nanofiber sample	Melting temperature (°C)
PVdF/PVP (Pure)	161.47
PVdF/PVP + 0.25 wt % carbon black	161.64
PVdF/PVP + 0.5 wt % carbon black	163.03
PVdF/PVP + 1 wt % carbon black	163.28
PVdF/PVP + 2 wt % carbon black	163.58
PVdF/PVP + 4 wt % carbon black	169.34

curves illustrate that the storage modulus decreases by increasing the temperature for all the samples; however, the reduction is not linear. It can be seen that after around 150 °C, the loss modulus of the samples with carbon black displayed a higher variation from the storage modulus especially at 4 wt % of carbon black. Figure 9 demonstrates that the storage modulus and loss modulus of all samples have a reduction by increasing the temperature; however the sample with 1 wt % carbon black showed the higher values up to 140–150 °C. In the PVdF/PVP sample with 4 wt % of carbon black, the loss modulus increased after 160 °C. Tan δ is the ratio of the loss modulus to the storage modulus which indicates the elasticity of the component. In addition, tan δ results of PVdF/PVP samples showed remarkable improvement by adding 1 wt % of carbon black but increasing the carbon black content decreased the values drastically; however, PVdF/PVP nanofiber in presence of 4 wt % carbon black displayed better result compare to pure PVdF/PVP sample. A high tan δ value demonstrates high nonelastic strain while low value indicates more elastic one.[38] The curves of the PVdF/PVP electrospun nanofibers show the higher value of tan δ for 1 wt % carbon black among all samples which exhibits the lower elastic strain; however, pure PVdF/PVP displayed the best elastic strain. The polymer network might be reinforced by adding carbon black up to 1 wt % that hinders the chain mobility of the PVdF, resulting in the reduction of the elasticity. Moreover, the addition of the 4 wt % carbon black decreases the tan δ value which denotes enhancing of the elastic properties of the membranes in elevated temperatures.

Effect of Annealing on Dielectric Constant Values

The dielectric constant values of PVdF/PVP nanofibers as a function of carbon black were determined at different annealing temperatures. Samples with different carbon black percentages were annealed to 90, 120, and 150 °C. Capacitance values were measured using an aluminum parallel-plate capacitor and power

Table II. Crystallinity of α-Phase PVdF/PVP Nanofibers

Nanofiber sample	Crystallinity (%)
PVdF/PVP (Pure)	52.44
PVdF/PVP + 0.25 wt % carbon black	56.74
PVdF/PVP + 0.5 wt % carbon black	62.02
PVdF/PVP + 1 wt % carbon black	67.91
PVdF/PVP + 2 wt % carbon black	54.15
PVdF/PVP + 4 wt % carbon black	54.59

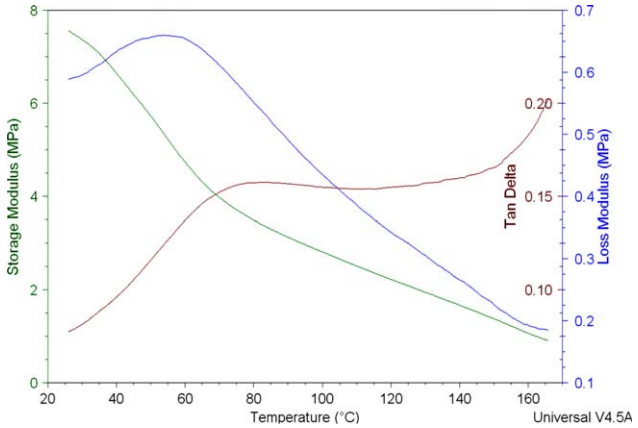

Figure 5. DMA curves of storage modulus, loss modulus, and tan δ of PVdF/PVP nanofiber. [Color figure can be viewed in the online issue, which is available at wileyonlinelibrary.com.]

supply. The dielectric constant ϵ_r can be obtained from the measured capacitance C by using the formula below[39]:

$$\epsilon_r = \frac{Cd}{A\epsilon_0} \quad (2)$$

where A is the cross-section area, d is the layer thickness, and ϵ_o is the vacuum dielectric constant. Figure 10 shows the dielectric constant values of PVdF/PVP nanocomposite fibers without and with annealing at 90, 120, and 150 °C. Results show that the addition of carbon black in PVdF/PVP nanofibers in all annealing conditions results in higher dielectric constants.

The measured dielectric constants of the nanocomposite fibers without annealing remarkably increased from 1.59 to 3.97 when the carbon black concentration reached 4 wt % in the PVdF/PVP nanocomposites. The annealed samples at 90 °C show better results compared to the PVdF/PVP nanofibers without annealing, as shown in Table III.

By enhancing the annealing temperatures from 120 to 150 °C, the dielectric constants increased slightly. PVdF/PVP with 4 wt % carbon black content annealed at 150 °C showed the highest value of 6.28. Improvement of the dielectric constants

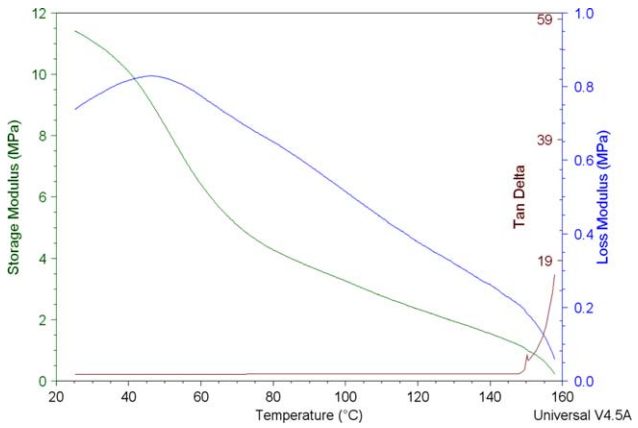

Figure 6. DMA curves of storage modulus, loss modulus, and tan δ of PVdF/PVP nanofiber with 1 wt % carbon black. [Color figure can be viewed in the online issue, which is available at wileyonlinelibrary.com.]

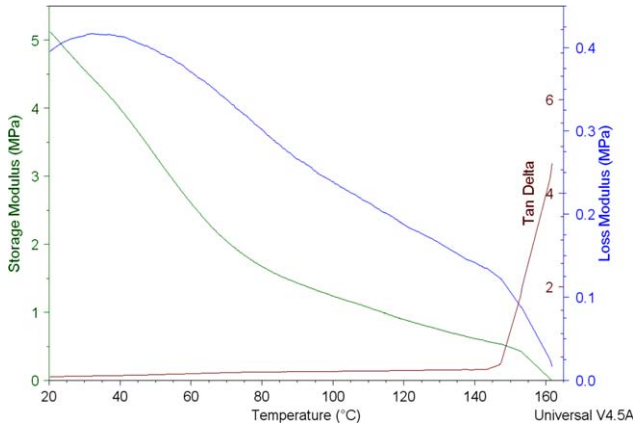

Figure 7. DMA curves of storage modulus, loss modulus, and tan δ of PVdF/PVP nanofiber with 2 wt % carbon black. [Color figure can be viewed in the online issue, which is available at wileyonlinelibrary.com.]

of the samples after annealing may have been due to the higher content of the β-phase (polar phase) in the structure because thermal treatment is one of the most common methods for transitioning from the nonpolar α-phase to the polar β-phase.[17,40] The highest improvement was obtained after adding 0.5 wt % carbon black into the structure at all annealing temperatures.

Effect of UV Exposure on Wettability

Polymerization and photo-polymerization are defined as the reaction of monomers to improve polymeric structures by UV light-induced initiation and then using the polymerization process. Energy radiation from UV light may excite the surface of fibers.[41] UV-induced surface modification has many advantages over other methods due to its low cost and simplicity. It is most important that UV-induced modification occurs mainly on the surface of membranes.[42,43] One of the most promising techniques to modify a membrane's surface is with the grafting method, which depends on the covalent bonding interaction of grafted chains. High-energy irradiation is controlled by polymerization with grafting of a single monomer or mixture of

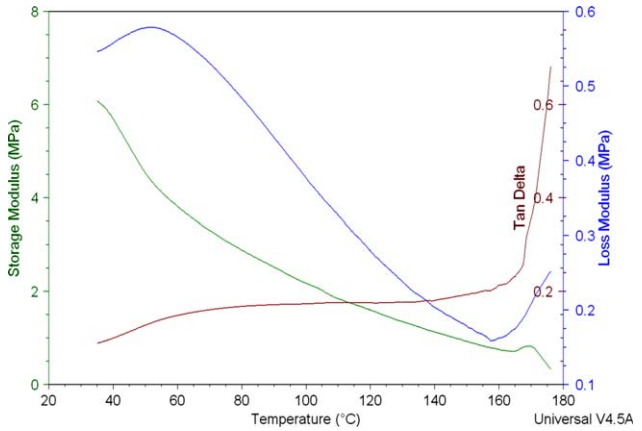

Figure 8. DMA curves of storage modulus, loss modulus, and tan δ of PVdF/PVP nanofiber with 4 wt % carbon black. [Color figure can be viewed in the online issue, which is available at wileyonlinelibrary.com.]

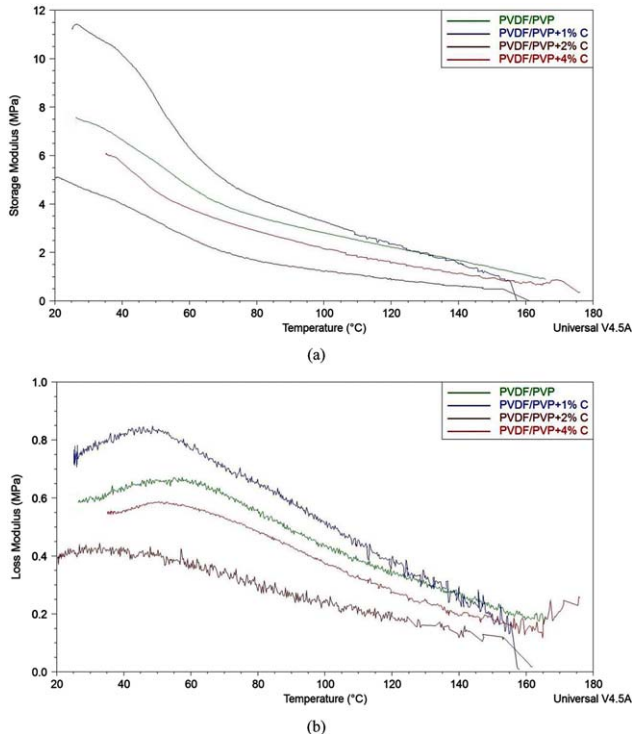

Figure 9. DMA curves, (a) storage modulus and (b) loss modulus of pure PVdF/PVP nanofiber, and incorporated with 1, 2, and 4 wt % carbon black. [Color figure can be viewed in the online issue, which is available at wileyonlinelibrary.com.]

two monomers.[44,45] Radical grafting with UV exposure to the surface of a PVdF membrane can render a hydrophilic feature with a highly wettable surface. It also improves the fouling resistance of PVdF membranes due to the increase of surface hydrophilicity.[46] Surface modification of PVdF is usually attained by grafting a functional layer or coating on the membrane surface.[47] The wettability of PVdF/PVP electrospun with different carbon black nanopowders content was examined as a function of UV irradiation time.

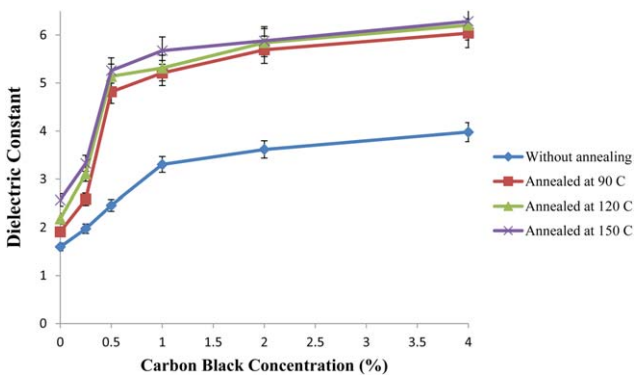

Figure 10. Dielectric constant values of PVdF/PVP fibers as a function of carbon black concentrations without and with annealing at 90, 120, and 150°C. [Color figure can be viewed in the online issue, which is available at wileyonlinelibrary.com.]

Table III. Dielectric Constants of Electrospun PVdF/PVP Nanofibers after Annealing at 90, 120, and 150 °C and Improvement Percentages

Annealing temperature (°C)	Carbon black concentration (wt %)	Dielectric constant	Improvement after annealing (%)
90	0	1.91	20
	0.25	2.58	31
	0.5	4.81	96
	1	5.20	58
	2	5.69	57
	4	6.03	52
120	0	2.18	37
	0.25	3.10	57
	0.5	5.13	109
	1	5.31	61
	2	5.84	62
	4	6.20	56
150	0	2.56	61
	0.25	3.32	68
	0.5	5.26	114
	1	5.67	72
	2	5.87	63
	4	6.28	58

The nanofiber samples were exposed to UV light as a function of irradiation time. Various times, from 5 to 20 days, were chosen for exposure to UV light. The PVdF/PVP nanofibers samples with 0, 0.25, 0.5, 1, 2, and 4 wt % of carbon black nanopowders were placed in a UV chamber for 5, 10, 15, and 20 days (Figure 11).

The contact angle values of samples were determined with a goniometer after each time period. Table IV shows the water contact angles of the PVdF/PVP nanofibers at different exposure times. These angles decreased by increasing the UV exposure time from 5 to 20 days. After 20 days, all samples showed a hydrophilic surface, and values of the contact angles were less than 90°. The high energy of irradiation after 20 days UV exposure caused surface grafting of the PVdF nanofibers. Figure 12 shows the changing of surface wettability of PVdF/PVP nanocomposites based on UV irradiation.

As can be seen, PVdF/PVP fiber with 4 wt % of carbon black content after 20 days UV exposure displayed the most improved wetting surface among other samples, with a contact angle of 37°. The contact angle measurements of the PVdF/PVP nanofibers by adding 1–4 wt % carbon black were slightly reduced for all UV exposure times.

Figure 11. PVdF/PVP electrospun nanofibers with 0, 0.25, 0.5, 1, 2, and 4 wt % of carbon black (right to left). [Color figure can be viewed in the online issue, which is available at wileyonlinelibrary.com.]

Table IV. Water Contact Angle Values of Electrospun PVdF/PVP Nanofibers as a Function of Carbon Black Concentrations before and after UV Exposure

UV exposure time	Carbon black concentration (wt %)	Water contact angle (°)
0 day	0	112
	0.25	111
	0.5	95
	1	81
	2	80
	4	78
5 days	0	102
	0.25	96
	0.5	85
	1	75
	2	72
	4	67
10 days	0	98
	0.25	93
	0.5	79
	1	68
	2	63
	4	58
15 days	0	97
	0.25	85
	0.5	75
	1	63
	2	55
	4	46
20 days	0	92
	0.25	79
	0.5	65
	1	56
	2	48
	4	37

Specific Capacitance Measurements

A Gamry instrument (Reference 600, Potentiostat/Galvanostat/ZRA) was utilized to characterize the specific capacitance of the electrospun nanofibers by using cyclic voltammetry. The PVdF/PVP samples with 0, 1, 2, and 4 wt % carbon black nanopowders were tested. An aqueous solution of 6M KOH, a common electrolyte for liquid supercapacitors,[48–50] was used in this experiment. The specific capacitance values are listed in Table V.The specific capacitance values of the PVdF/PVP nanofibers increased significantly by adding carbon black nanopowders from 0.233 to 2.544 Fg^{-1}. No major difference was seen between the values where 2 and 4 wt % carbon black was

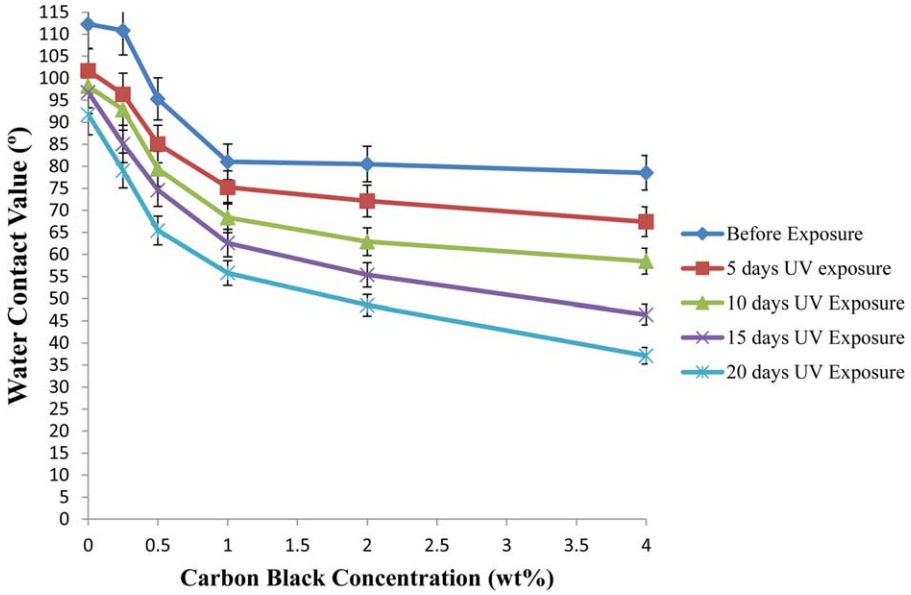

Figure 12. Surface wettability of PVdF/PVP nanocomposite fibers as a function of carbon black concentrations after different UV exposure times. [Color figure can be viewed in the online issue, which is available at wileyonlinelibrary.com.]

Table V. Specific Capacitances of PVdF/PVP Nanofibers

Nanofiber sample	Specific capacitance (Fg^{-1})
PVdF/PVP (Pure)	0.233
PVdF/PVP + 1 wt % carbon black	1.560
PVdF/PVP + 2 wt % carbon black	2.146
PVdF/PVP + 4 wt % carbon black	2.544

added. Improving the specific capacitance may be due to the high conductivity of carbon black. A similar study was done by Ortega *et al.*,[24] reported specific capacitance of around 41 Fg^{-1} for gel polymer electrodes (GPE) containing PVdF.

CONCLUSIONS

PVdF-based polymeric nanocomposite fibers incorporated with different weight percentages of carbon black nanoparticles were fabricated via the electrospinning process. The sizes of all PVdF/PVP nanofibers were between 100 and 200 nm. The DSC results show the endothermic peaks, melting temperatures, and crystallinity of nanofibers with different percentages of carbon black nanoparticles. The TGA results demonstrate that the addition of carbon black into the polymer matrix does not appreciably improve the thermal stability and the weight loss pattern and corresponding temperatures are almost similar to PVdF/PVP nanofibers. The DMA results indicate that the storage modulus and loss modulus values of nanocomposite fibers with different carbon black content were remarkably increased compared to the pure PVdF/PVP samples. The dielectric constant values of the fibers were considerably improved by annealing the samples to 150 °C. Energy radiation using the UV light enhanced the surface wetting properties of the samples. The specific capacitance of the PVdF/PVP electrospun membranes reached to a maximum level by adding 4 wt % of carbon black nanoparticles. This study exhibited that the electrospun nanofibers have superior thermal, mechanical and other physical properties, which may be useful for the applications of supercapacitor separators and other energy storage devices.

ACKNOWLEDGMENTS

The authors gratefully acknowledge the Kansas NSF EPSCoR (#R51243/700333), and Wichita State University for the financial and technical support of this work.

REFERENCES

1. Aravindan, V.; Cheah, Y. L.; Mak, W. F.; Wee, G.; Chowdari, B. V. R.; Madhavi, S. *Chem. Plus Chem.* **2012**, *77*, 570.
2. Zhou, Z.; Lai, C.; Zhang, L.; Qian, Y.; Hou, H.; Reneker, D. H.; Fong, H. *Polymer* **2009**, *50*, 2999.
3. Kim, C.; Kim, J. S.; Kim, S. J.; Lee, W. J.; Yang, K. S. *J. Electrochem. Soc.* **2004**, *151*, A769
4. Xu, B.; Yue, S.; Sui, Z.; Zhang, X.; Hou, S.; Cao, G.; Yang, Y. *Energy Environ. Sci.* **2011**, *4*, 2826.
5. Pandolfo, A. G.; Hollenkamp, A. F. *J. Power Sources* **2006**, *157*, 11.
6. Wee, G.; Soh, H. Z.; Cheah, Y. L.; Mhaisalkar, S. G.; Srinivasan, M. *J. Mater. Chem.* **2010**, *20*, 6720.
7. Shiang, T.; Gene, S.; Wei, W.; Ashutosh, T. *Electrochem. Solid-State Lett.* **2014**, *2*, M25.
8. Yang, K. S.; Joo, Y. W.; Kim, C.; Kim, J. H.; Lee, W. J. "Performances of Electrochemical Hybrid Supercapacitor of RuO_2/Activated Carbon Nanofibers from Electrospinning," Proc. 3rd WSEAS/IASME International Conference on Electroscience and Technology for Naval Engineering, Greece, **2006**, pp 6–10.

9. Heon, M.; Liofland, S.; Applegate, J.; Notle, R.; Cortes, E.; Hettinger, J. D.; Taberna, P. L.; Simon, P.; Huang, P.; Brunet, M.; Gogotsi, Y. *Energy Environ. Sci.* **2011**, *4*, 135.
10. Zhu, Y.; Murali, S.; Stoller, M. D.; Ganesh, K. J.; Cai, W.; Ferreira, P. J.; Pirkle, A.; Wallace, R. M.; Cychosz, K. A.; Thommes, M.; Su, D.; Stach, E. A.; Ruoff, R. S. *Science* **2011**, *332*, 1537.
11. Heikkila, P.; Harlin, A. *Eur. Polym. J.* **2008**, *44*, 3067.
12. Varesano, A.; Carletto, R. A.; Mazzuchetti, G. *J. Mater. Process. Technol.* **2009**, *209*, 5178.
13. Kim, J. R.; Choi, S. W.; Jo, S. M.; Lee, W. S.; Kim, B. C. *Electrochim. Acta* **2004**, *50*, 69.
14. Periasamy, P.; Tatsumi, K.; Shikano, M.; Fujieda, T.; Saito, Y.; Sakai, T.; Mizuhata, M.; Kajinami, A.; Deki, S. *J. Power Sources* **2000**, *8*, 269.
15. Kim, Y. W.; Lee, D. K.; Lee, K. J.; Kim, J. H. *Eur. Polym. J.* **2008**, *44*, 932.
16. Chen, G. X.; Li, L. I.; Shimizu, H. *Carbon* **2007**, *45*, 2334.
17. Zheng, J.; He, A.; Li, J.; Han, C. C. *Macromol. Rapid Commun.* **2007**, *28*, 2159.
18. Beck, F.; Dolata, M.; Grivei, E.; Probst, N. *J. Appl. Electrochem.* **2001**, *31*, 845.
19. Lewandowski, A.; Zajder, M.; Frackowiak, E.; Beguin, F. *Electrochim. Acta* **2001**, *46*, 2777.
20. Sivaraman, P.; Rath, S. K.; Hande, V. R.; Thakur, A. P.; Patri, M.; Samui, A. B. *Synth. Met.* **2006**, *156*, 1057.
21. Miao, J.; Miyauchi, M.; Simmons, T. J.; Dordick, J. S.; Linhardt, R. J. *J. Nanosci. Nanotechnol.* **2010**, *10*, 5507.
22. Karabelli, D.; Leprêtre, J. C.; Alloin, F.; Sanchez, J. Y. *Electrochim. Acta* **2011**, *57*, 98.
23. T. J. Simmons, Carbon Nanotube Suspensions, Dispersions and Composites; PhD dissertation, Dept. of Chemistry, Rensselaer Polytechnic Institute, New York, **2008**.
24. Ortega, P. F. R.; Trigueiro, J. P. C.; Silva, G. G.; Lavall, R. L. *Electrochim. Acta* **2015**, *188*, 809.
25. Ketpang, K.; Park, J. S. *Synth. Met.* **2010**, *160*, 1603.
26. Chen, D.; Wang, M.; Zhang, W. D.; Liu, T. *J. Appl. Polym. Sci.* **2009**, *113*, 644.
27. Jin, Z.; Pramoda, K. P.; Goh, S. H.; Xu, G. *Mater. Res. Bull.* **2002**, *37*, 271.
28. Li, Z.; Shan, F.; Wei, J.; Yang, J.; Li, X.; Wang, W. *J. Solid State Electrochem.* **2008**, *12*, 1629.
29. Golcuk, S.; Muftuoglu, A. E.; Celik, S. U.; Bozkurt, A. *J. Polym. Res.* **2013**, *20*, 1.
30. Salami, A.; Yousefi, A. A. *Polym. Test.* **2003**, *22*, 699.
31. Campos, J. S. D. C.; Ribeiro, A. A.; Cardoso, C. X. *Mater. Sci. Eng. B* **2007**, *136*, 123.
32. Lawrence, J. *Thermochim. Acta* **2006**, *442*, 92.
33. Magniez, K.; De Lavigne, C.; Fox, B. L. *Polymer* **2010**, *51*, 2585.
34. Silva, M. P.; Costa, C. M.; Sencadas, V.; Paleo, A. J. *J. Polym. Res.* **2011**, *18*, 1451.
35. Chen, N.; Hong, L. *Polymer* **2002**, *43*, 1429.
36. Huang, J. C. *Adv. Polym. Tech.* **2002**, *21*, 299.
37. Linares, A.; Acosta, J. L. *Eur. Polym. J.* **1997**, *33*, 467.
38. Santos, C.; Silva, C. J.; Buttel, Z.; Guimaraes, R.; Pereira, S. B.; Tamagnini, P.; Zille, A. *Carbohydr. Polym.* **2014**, *99*, 584.
39. Khan, W. S.; Asmatulu, R.; El-Tabey, M. M. *J. Nanotechnol. Eng. Med.* **2010**, *1*, 6.
40. Dillon, D. R.; Tenneti, K. K.; Li, C. Y.; Ko, F. K.; Sics, I.; Hsiao, B. S. *Polymer* **2006**, *47*, 1678.
41. Asano, M.; Chen, J.; Maekawa, Y.; Sakamura, T.; Kubota, H.; Yoshida, M. *J. Polym. Sci. A: Polym. Chem.* **2007**, *45*, 2624.
42. Ulbricht, M.; Matuschewski, H.; Oechel, A.; Hicke, H. G. *J. Membr. Sci.* **1996**, *115*, 31.
43. Brink, L. E. S.; Elbers, S. J. G.; Robbertsen, T.; Both, P. *J. Membr. Sci.* **1993**, *76*, 281.
44. Kato, K.; Uchida, E.; Kang, E. T.; Uyama, Y.; Ikada, Y. *Prog. Polym. Sci.* **2003**, *28*, 209.
45. Bhattacharya, A.; Misra, B. N. *Prog. Polym. Sci.* **2004**, *29*, 767.
46. Akhtar, S.; Hawes, C.; Dudley, L.; Reed, I.; Strathford, P. *J. Membr. Sci.* **1995**, *107*, 209.
47. Liu, F.; Hashim, N. A.; Liu, Y.; Moghareh Abed, M. R.; Li, K. *J. Membr. Sci.* **2011**, *375*, 1.
48. Kim, B. H.; Yang, K. S.; Woo, H. G.; Oshida, K. *Synth. Met.* **2011**, *161*, 1211.
49. Li, J.; Liu, E. H.; Li, W.; Meng, X. Y.; Tan, S. T. *J. Alloys Compounds* **2009**, *478*, 371.
50. Khan, W. S.; Asmatulu, R.; Rodriguez, V.; Ceylan, M. *Int. J. Energy Res.* **2014**, *38*, 2044.